Mechanics & Industry **23**, 14 (2022)

https://doi.org/10.1051/meca/2022008

Mechanics & Industry

Available online at:
www.mechanics-industry.org

REGULAR ARTICLE

OPEN ACCESS

Experimental study on influence of ultrasonic vibration on forming limit

Changli Zha* and Shenlong Zha

School of Electronic Engineering and Intelligent Manufacturing, Anqing Normal University, Anhui 246133, PR China

Received: 25 September 2021 / Accepted: 15 March 2022

Abstract. Applying ultrasonic vibration in sheet metal forming can change its forming mechanism and improve its formability. The uniaxial tensile and bulging forming limit experimental setups were designed to study the ultrasonic vibration and forming limit relationship induced by ultrasonic excitation, and the results under different experimental conditions were analyzed. It was found that ultrasonic vibration has different effects on the left and right sides of forming limit diagram (FLD). Under the same ultrasonic vibration frequency, the maximum increment of left and right major limit strain is about 9.3% and 8.7%, respectively. The former is larger than the latter, and the strain increment increases with the increase of ultrasonic vibration frequency, but the basic shapes of FLD are unchanged.

Keywords: Ultrasonic vibration / uniaxial tension / bulging / forming limit diagram

1 Introduction

The introduction of ultrasonic vibration into metal plastic forming decreases forming force and friction [1] and effectively prevents wrinkling and tearing [2]. Therefore, ultrasonic vibration is applied to plastic forming processes, such as wiredrawing [3], tube-drawing [4], and extrusion [5]. Ultrasonic vibration will alter the sheet forming mechanism and process parameters during metal sheet forming, thus improving forming performances. The forming limit is an important process parameter of metal sheet forming and a key indicator for evaluating forming performance. Furthermore, the forming limit reflects the limit deformation degree before the failure of metal sheet forming. Based on the M-K groove theory, Banabic D [6,7] introduced physical vibration parameters and built a forming limit prediction model under vibration conditions. The theoretical prediction and experimental results of forming limit were compared through drawing experiments with HPC35 Al alloy materials, and it was found that vibration significantly affected forming limit diagrams (FLDs). Similarly, Najafizadeh et al. [8] validated the role of ultrasonic vibration in rigid hemispherical punch bulging experiments of St14 steel plates. Though some researchers experimentally studied the effects of ultrasonic vibration on forming limit, the existing research was limited to analyzing a single experimental phenomenon without FLD to predict forming performance in practice.

The uniaxial tensile and bulging forming limit experimental system was modified in this study. Then effects of ultrasonic vibration on metal sheet forming limit were explored under different specimen sizes and ultrasonic vibration parameters. Relevant experimental data and FLDs were obtained to study correlations between ultrasonic vibration and metal sheet FLD. The results will provide criteria for predicting metal plastic forming performances assisted by ultrasonic vibration in practice.

2 Experimental analysis

Conventional metal sheet forming limit test methods mainly include non-planar deformation [9] and planar measurement [10–12]. Since friction at the mesoscopic scale is impacted by the scale effect, during selection and designing of forming limit measuring method and instrument, attention should be paid to avoid measuring errors due to the scale effect and die precision, which otherwise will affect the true experimental results. Thus, as for mesoscopic metal sheet forming limit experiments based on ultrasonic vibration, the precision errors caused by mesoscopic scale effect and die scale proportional diminution were considered. The FLD is the most commonly used fracture criterion for sheet metal forming applications, which is shows the amount of deformation (strain) a sheet material can resist as function of the deformation mode and is a relation between the major and minor strain (Fig. 1). As shown in Figure 1, the FLD was drawn according to the experimental data obtained by uniaxial tensile [13] and Nakajima hemisphere rigid punch bulging tests [10].

* e-mail: 504275049@qq.com

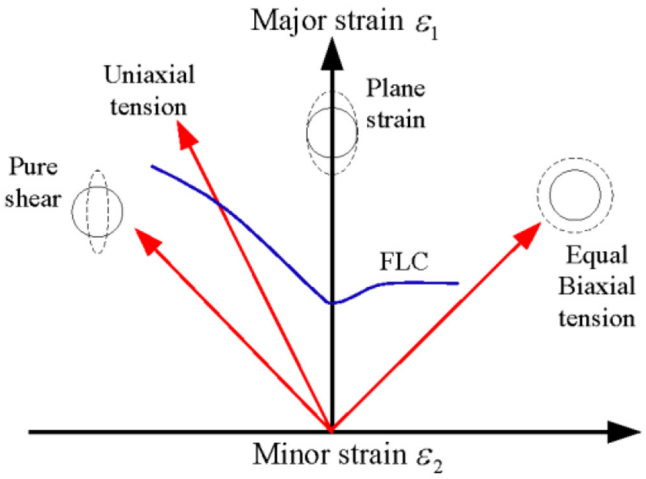

Fig. 1. Forming limit diagram [14].

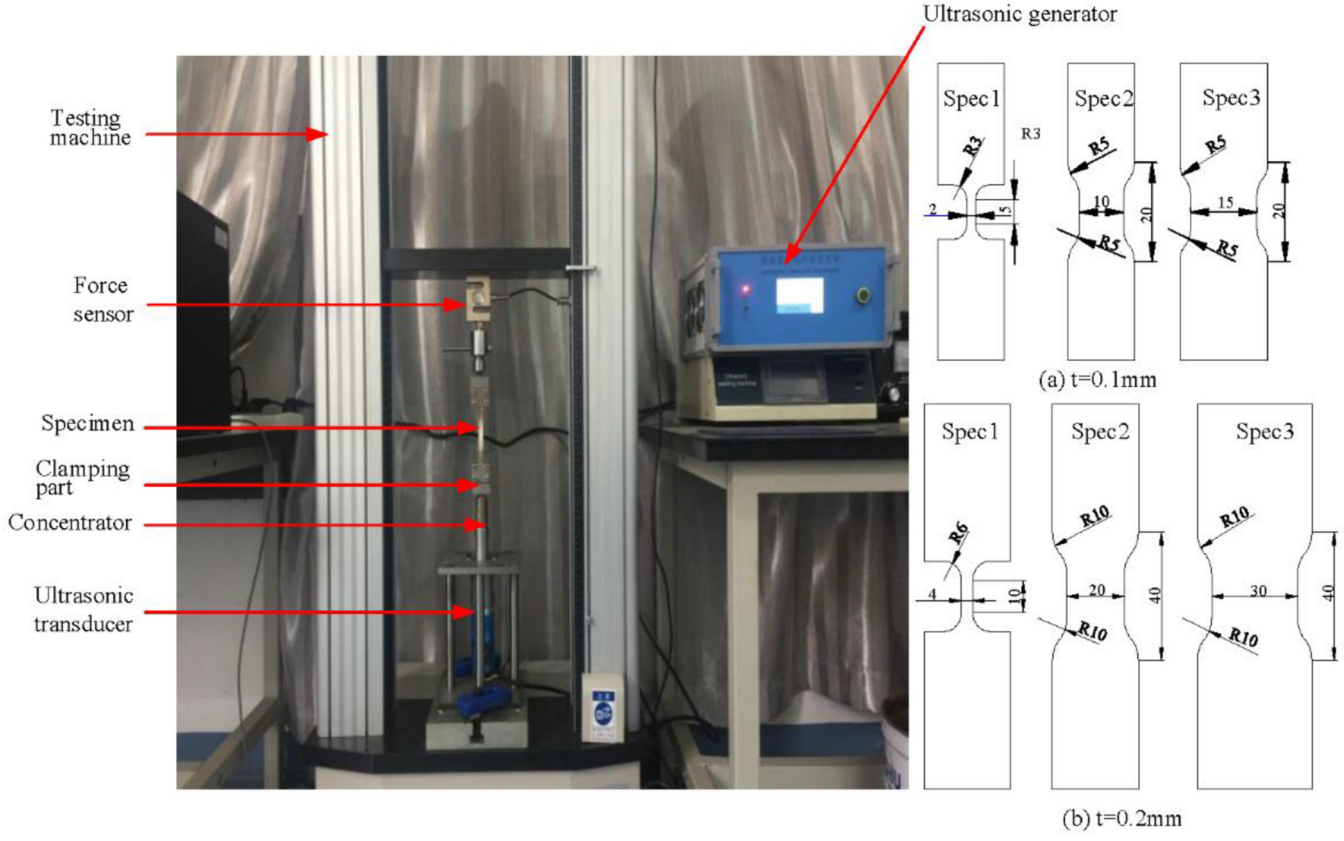

Fig. 2. Uniaxial tensile testing device of forming limit based on ultrasonic vibration.

3 Uniaxial tensile experiments

To acquire accurate and detailed experimental data at the left side of metal sheet FLDs (i.e., major strain ε_1, minor strain ε_2), specimens in two different thicknesses were selected. Each thickness corresponded to specimens in three different sizes (Spec1, Spec2, and Spec3). Consequently, the strain path was altered to form different proportions of major strain ε_1 to minor strain ε_2. The experimental data at the left side of FLDs were analyzed. The forming limit tensile test device of a mesoscopic metal sheet based on ultrasonic vibration is illustrated in Figure 2.

The device consists of an ultrasonic vibration unit, a control system, force sensors, and a test machine. The ultrasonic vibration unit is comprised of an ultrasonic

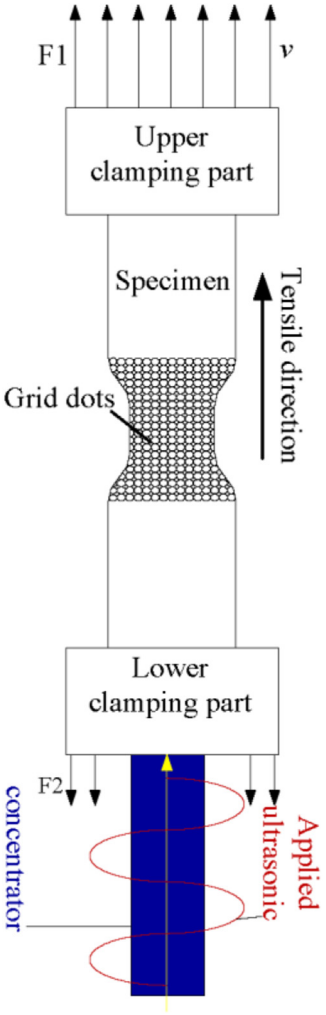

Fig. 3. Uniaxial tensile experimental principle of forming limit based on ultrasonic vibration.

generator, an ultrasonic transducer, and a concentrator. Specifically, the ultrasonic generator can output at an operating frequency of 20-25 kHz with a peak output power of 2 kW. The specimens were applied with three different operating frequencies to study the effects of ultrasonic vibration on the forming limit of metal sheets. The specimen was clamped by the upper and lower clamping part and installed in the working area of the tensile testing machine, and the ultrasonic wave was transmitted to the specimen through the lower clamping part. The experimental principle is illustrated in Figure 3. The test machine is a power supply in the experiments. The real-time tensile forces of the specimens during tension were recorded by sensors and delivered to the control system. The specimens were polished, cleaned, and made into surface-printed grids by an electrochemical corrosion method. The major axis and minor axis strains of grid dots after deformation were measured using an electron microscope. Before experiments, the fracture force points were pre-tested to optimize the fracture positions of the specimens and to improve the measurement accuracy of strains. Furthermore, the

Table 1. Chemical composition of SUS304.

Brand (name)	C%	Si%	Mn%	P%	S%	Ni%	Cr%
SUS304	0.08	0.75	2	0.045	0.03	8-10.5	18-20

Table 2. Experimental parameters.

Parameter	Value
Testing machine (kN)	50
Tensile working velocity (mm/s)	0.01
Specimen thickness (mm)	0.1
	0.2
	20
Work frequency (kHz)	21.5
	23.5

experiments of each specimen were repeated at least 3 times under each scheme to ensure the effectiveness of the experimental results.

3.1 Experimental parameters

To measure the data at the left side of FLDs, SUS304 stainless steel (chemical composition listed in Tab. 1) sheets of different thicknesses and sizes were selected for uniaxial tensile experiments. The effects of ultrasonic vibration at different applied frequencies on forming limit were explored. Given the rigid plasticity of SUS304 stainless steel sheets, small tensile working velocity (microscopic tension) and low strain rate were selected to acquire high-precision experimental data. The working parameters are listed in Table 2.

3.2 Results and analysis

3.2.1 Without ultrasonic vibration

Firstly, micro tensile forming limit experiments were carried out on the specimens in three sizes without ultrasonic vibration. Then, specimens were observed using an electron microscope and an image measuring system for major and minor strain measurement in coordinate grids.

It can be seen from Figure 4a that the limit strain of spec1 deviates slightly from the planar strain. The reason was that the effect of excessive fillet radius on strain path decreased, and the decreasing grain number in sections due to smaller width and thickness aggravated the strain gradient hardening effect. The limit strain of spec3 was basically consistent with the designed strain path $\varepsilon_1 = -2\varepsilon_2$, as shown in Figure 4c. However, the limit strain path of spec2 was between those of spec1 and spec3, as shown in Figure 4b. Furthermore, the limit strain of 0.2 mm-thick specimens generally surpassed that of 0.1 mm-thick specimens because the increased specimen size increased the forming limit.

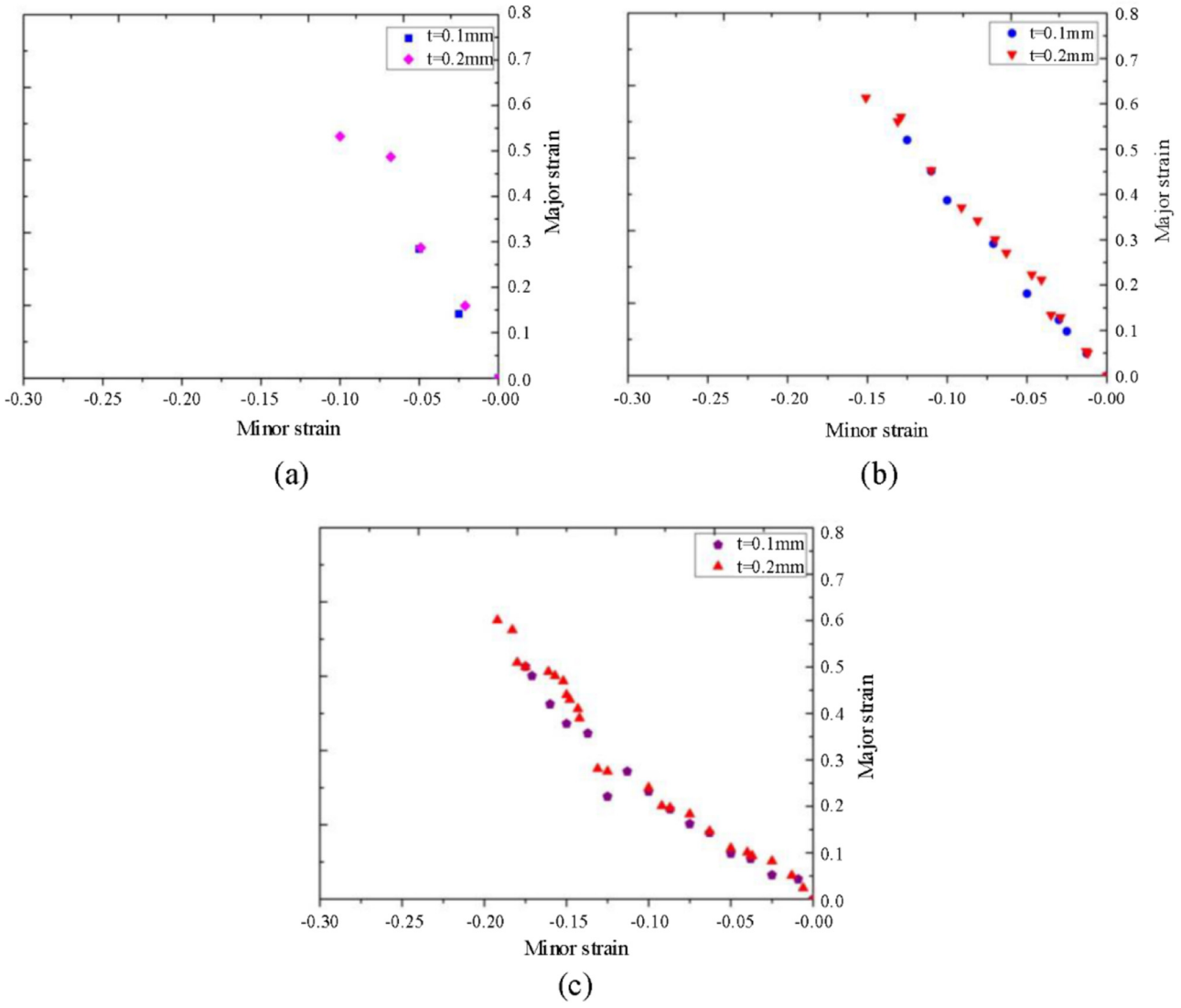

Fig. 4. Limit strain of different specimens without ultrasonic vibration. (a) spec1. (b) spec2. (c) spec3.

3.2.2 Applied ultrasonic vibration

Based on the above experiments with ultrasonic vibration, the micro tensile experiments of specimens in each size (spec1, spec2, spec3) were assisted by ultrasonic vibration at the three frequencies (20, 21.5, 23.5 kHz) separately. To ensure comparability of experimental data, external position sensors were used to trigger the ultrasonic generator at the same position so that ultrasonic vibration was applied at the same position during the experiments. Then the measured data were processed and analyzed.

The limit strain of specimens was significantly affected by ultrasonic vibration, and the effect increased with the increase of ultrasonic vibration frequency. The limit strain curves show that ultrasonic vibration slightly affects spec1, as shown in Figure 5a. The reason was that the internal metallographic structure of spec1 was not severely softened under ultrasonic vibration due to the smaller size [15]. Therefore, the increment gradient of limit strain on the small-section fractures decreased. As the sizes increased, softening effect (i.e., volume effect) due to ultrasonic vibration is more severe, resulting in the significant increment of limit strain, as shown in Figure 5b and c. Further comparative analysis showed the changing amplitudes of limit strains under ultrasonic vibration at different frequencies, as shown in Figure 6.

The ranges of limit strain increment from specimens at two thicknesses and three sizes were analyzed under three different frequencies. As the vibration frequency rises from 20 to 23.5 kHz, the limit strain increment at the thickness $t = 0.1$ and 0.2 mm varies within 2–4% and 2.5–4.4%, respectively, as shown in Figure 6a. As shown in Figure 6b, the limit strain increment at the thickness $t = 0.1$ and 0.2 mm varies within 2.2–4.3% and 2.8–5.1%, respectively. As shown in Figure 6c, the limit strain increment at the thickness $t = 0.1$ and 0.2 mm varies within 2.7–5.1% and 4.1–9.3%, respectively.

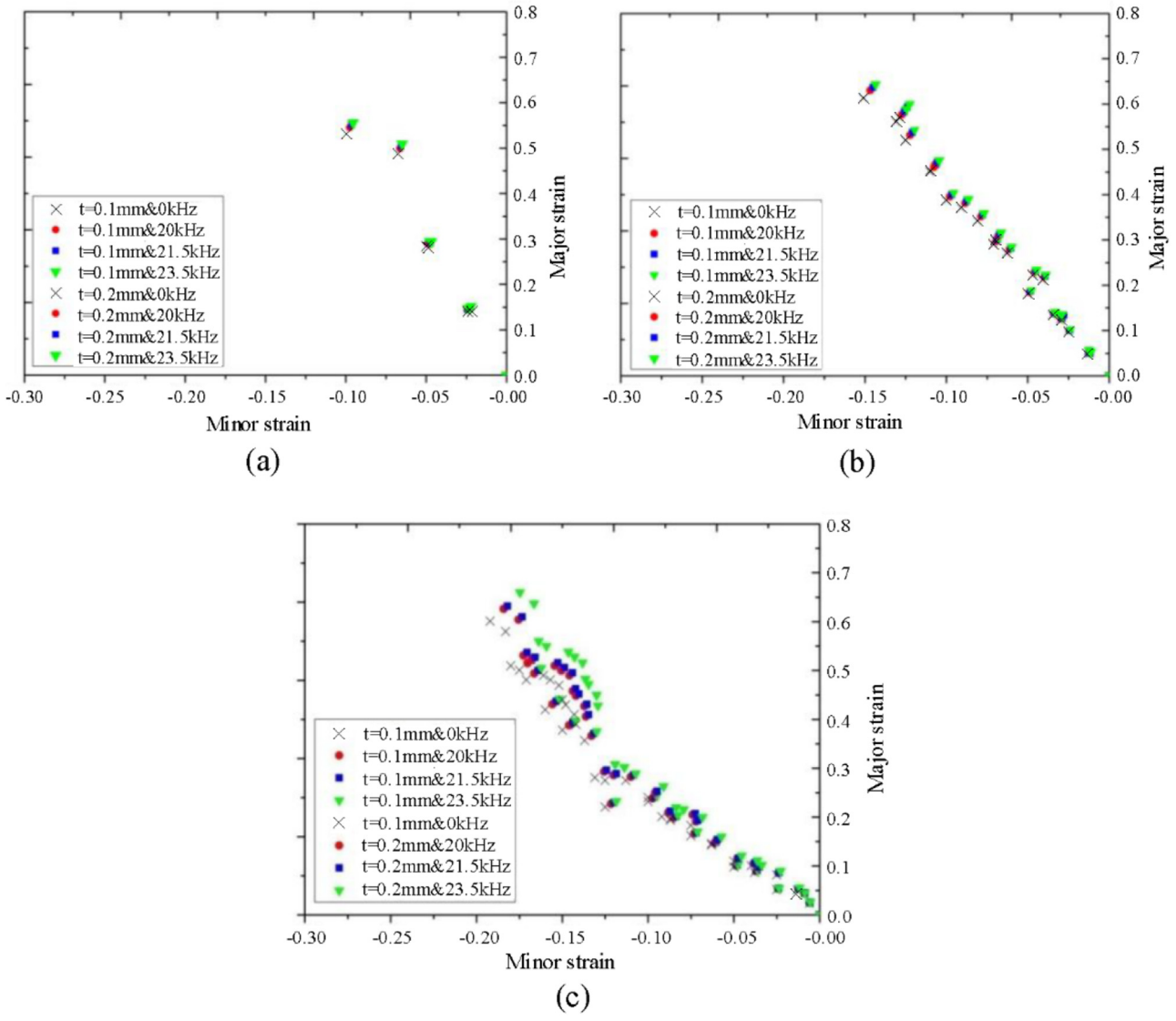

Fig. 5. Limit strain of different specimens under ultrasonic vibration. (a) spec1. (b) spec2. (c) spec3.

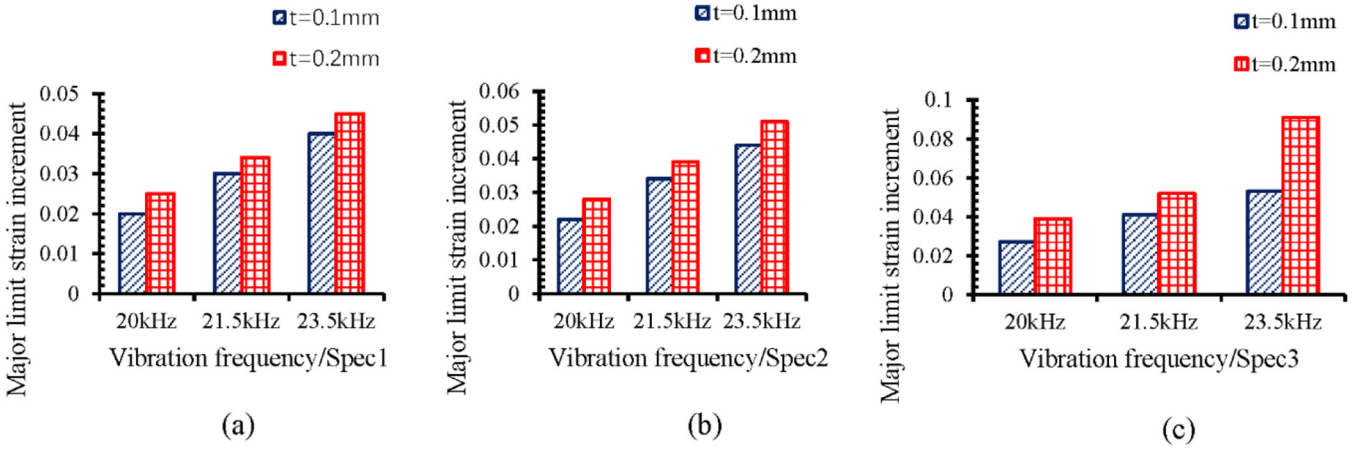

Fig. 6. Limit strain increment of specimens with different frequencies. (a) spec1. (b) spec2. (c) spec3.

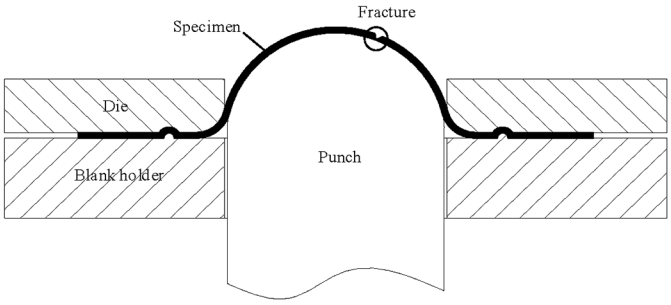

Fig. 7. Experimental schematic diagram of Nakajima rigid hemispherical punch Bulge-Forming.

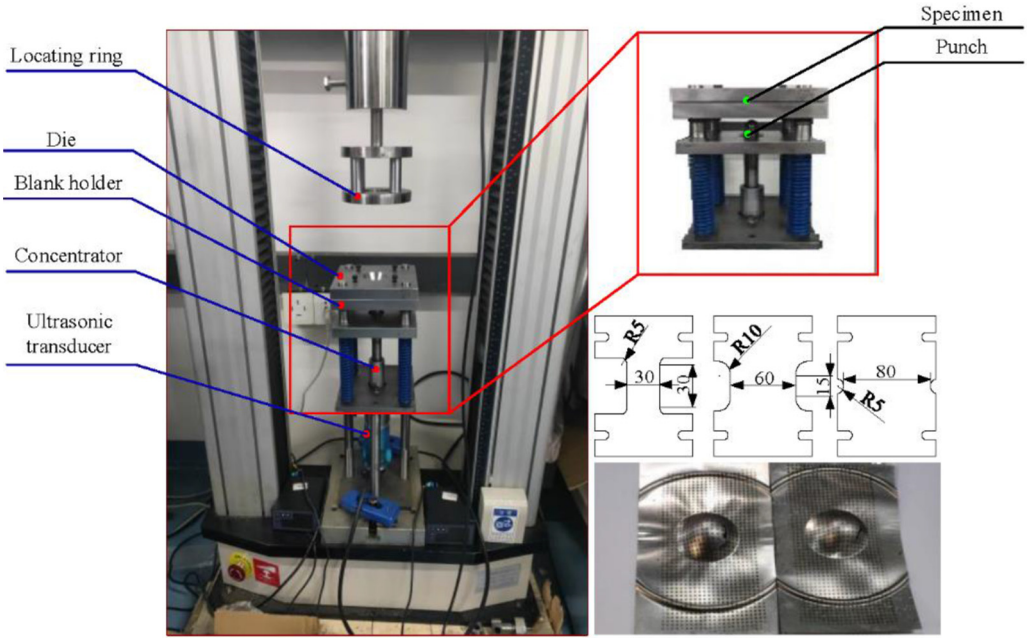

Fig. 8. The experimental device of bulging-forming based on ultrasonic vibration.

4 Bulging experiments

The experimental schematic diagram of Nakajima hemisphere rigid punch bulging [10] is illustrated in Figure 7. Specifically, metal sheets within a certain thickness range were fixed between a die and a blank holder and then were punched and bulged by a rigid hemispherical punch. These treatments were stopped immediately upon the occurrence of fracturing. Then the coordinate grid major axis and minor axis (namely major strain ε_1 and minor strain ε_2) at the position of fracturing were measured. The deformation mode of metal sheets were transited from uniaxial tension to biaxial tension through the variation of specimen sizes. Finally, experimental data at the right side of FLD were acquired.

The bulging forming limit experiment platform based on ultrasonic vibration was a modified Nakajima rigid hemispherical punch bulging system. Specifically, ultrasonic vibration was introduced into the punching bulging process. The platform mainly consists of an ultrasonic vibration unit, a control system, and a test machine. The ultrasonic vibration unit is comprised of an ultrasonic generator, an ultrasonic transducer, and a concentrator. Given the generality of the platform and the principle of low energy consumption, threads were adopted to connect the amplitude transformer and the punch-bulging punch directly. The punch transferred ultrasonic vibration to the tested specimen during punch bulging. The working velocity of punch bulging was set by the control system. To ensure the precision of experimental data, the working velocity was set at 0.01 mm/s, and the fracture position was optimized, thus improving the reliability and precision of experimental data. Specimens with a thickness of 0.2 mm and different sizes (spec1, spec2, spec3) were designed to alter the strain path. The specimens in each size were processed both with and without ultrasonic vibration. The three ultrasonic vibration frequencies (20, 21.5, 23.5 kHz) are the same as those in the micro tensile forming experiments. The coordinate grid major and minor axes of specimens after punch bulging were measured using an ARGUS strain measuring system for higher measurement accuracy. The improved bulging forming limit testing

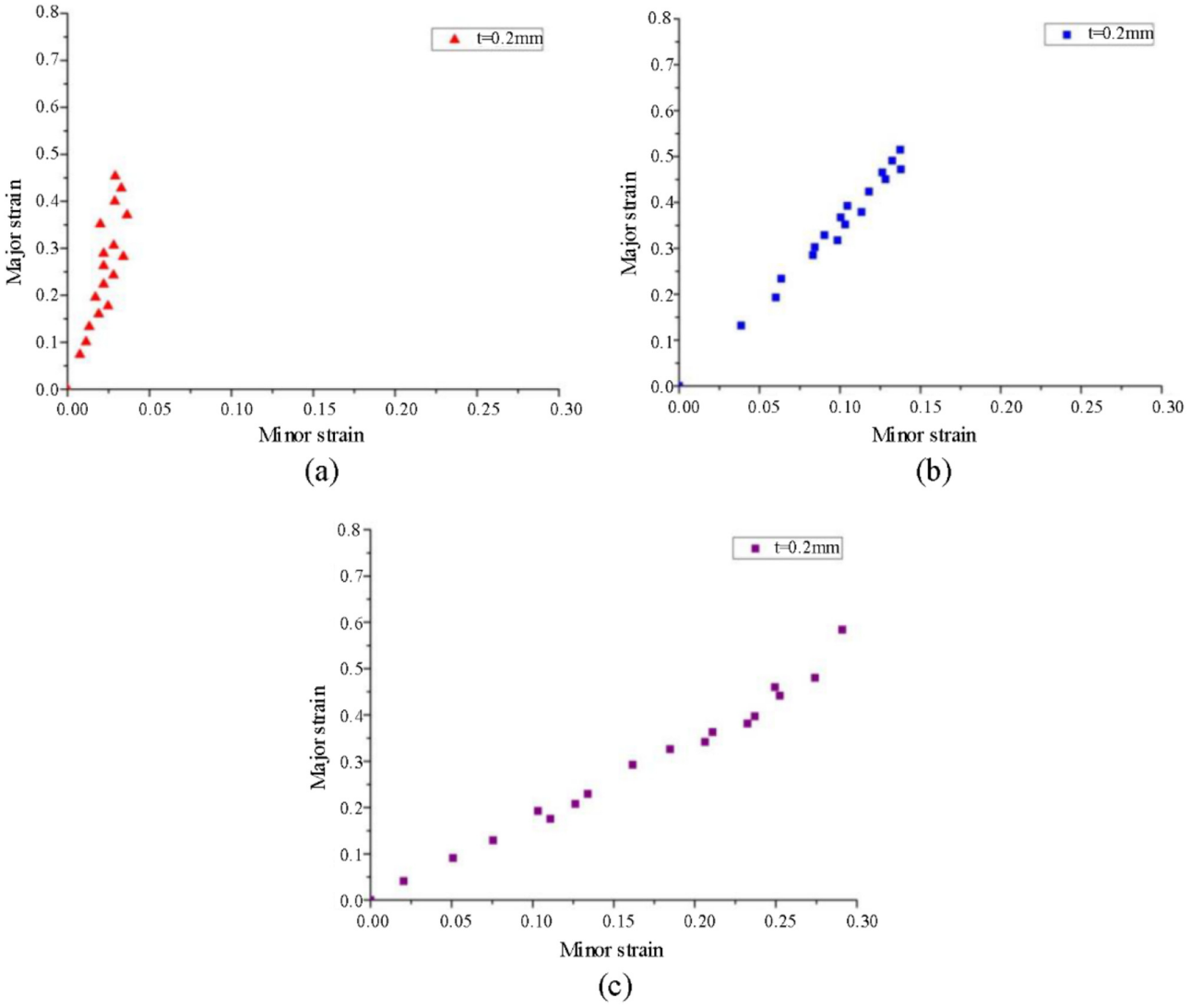

Fig. 9. Bulging-forming limit strain of different specimens without ultrasonic vibration. (a) spec1. (b) spec2. (c) spec3.

platform based on ultrasonic vibration is illustrated in Figure 8.

4.1 Results and analysis

4.1.1 Without ultrasonic vibration

To decrease the impact of friction on the results of punch bulging experiments, the rigid hemispherical punch specimens were surface-lubricated by grease in each experiment. Spring was installed between the blank holder and base. The blank holder force was adjusted by adjusting the working stroke of the limit bolt to provide appropriate blank holder force and avoid wrinkling during punch bulging. Furthermore, drawbead was designed to ensure successful operations further. Positioning rings were designed above the dies to ensure the positional precision of different parts during punch forming. Before the punch bulging experiments, the specimens were polished to avoid measurement errors caused by cracks, burrs or roughness on specimen edges. The specimens of each size were measured using the ARGUS strain measuring system and were repeated at least 3 times to ensure the accuracy of experimental data. The results are shown in Figure 9.

Figure 9 shows that the limit strain of spec1 to spec3 transited from planar strain to a biaxial status with increasing limit strain. The limit strain of spec3 was basically consistent with the designed strain path $\varepsilon_1 = \varepsilon_2$, and the limit strain path of spec1 was basically consistent with the planar strain path. The forming limit major strain obtained by rigid hemispherical punch bulging was generally smaller than that obtained by tensile tests. The main cause for such phenomenon was that the forming limit minor strain under biaxial tensile stress was enlarged.

4.1.2 Applied ultrasonic vibration

Three vibration frequencies (20, 21.5, 23.5 kHz) were applied during punch bulging experiments, and the specimens of each size (spec1, spec2, spec3) were processed by ultrasonic vibration-assisted punch bulging at the

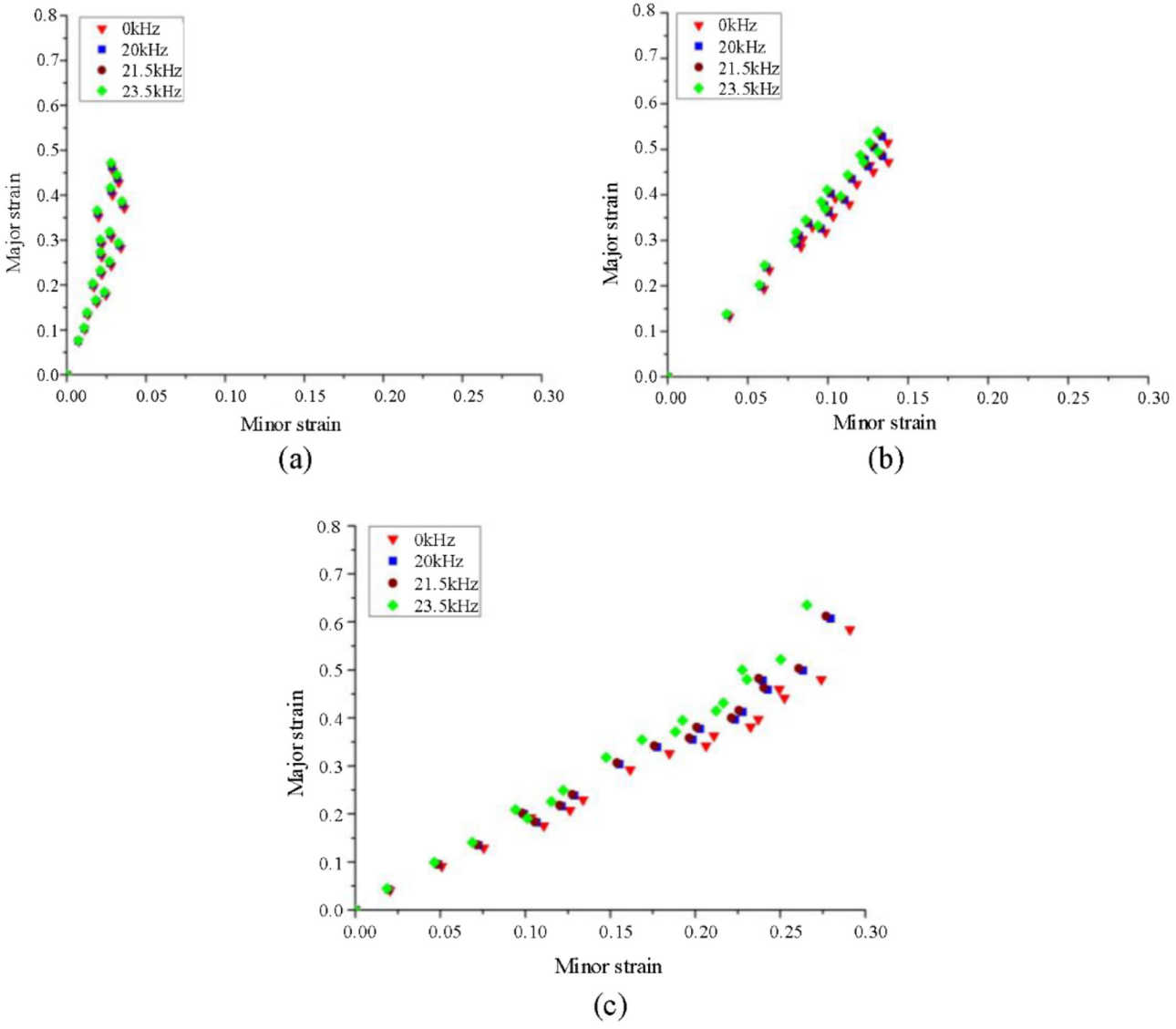

Fig. 10. Bulging-forming limit strain of different specimens under ultrasonic vibration. (a) spec1. (b) spec2. (c) spec3.

three frequencies. The processed data are illustrated in Figure 10.

From the above figures, the limit major strain of specimens was significantly affected by the ultrasonic vibration and increased with the increase of ultrasonic vibration frequency. The limit major strain of spec1 was the least affected by ultrasonic vibration, while spec3 was the most sensitive to ultrasonic vibration. However, compared with tensile forming experiments, the influence of ultrasonic vibration on forming limit was smaller. The major reason was that unavoidable friction occurred during experiments. The specific range in punch bulging limit major strain increment of specimens under ultrasonic vibration is shown in Figure 11.

As shown in Figure 11, the ranges of limit strain increment from specimens at three sizes were analyzed under three different frequencies. As the vibration frequency rises from 20 to 23.5 kHz, the limit strain increment increase with the increase of vibration frequency, and varies within 1.9–8.7%.

5 Correlations between ultrasonic vibration and forming limit curves

The limit strains of specimens in different sizes and under different vibration frequencies were measured through uniaxial tensile tests and rigid hemispherical punch bulging experiments. Therefore, the corresponding forming limit points were determined. According to the forming limit points under different strain paths, the FLDs of the metal sheets without or with ultrasonic vibration were plotted. The FLDs of 0.2 mm-thick SUS304 sheets with or without ultrasonic vibration are shown in Figure 12.

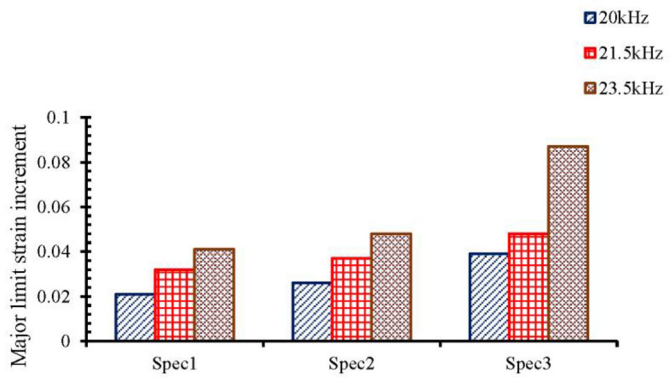

Fig. 11. Limit major strain increment of bulging-forming for three specimens under different frequencies.

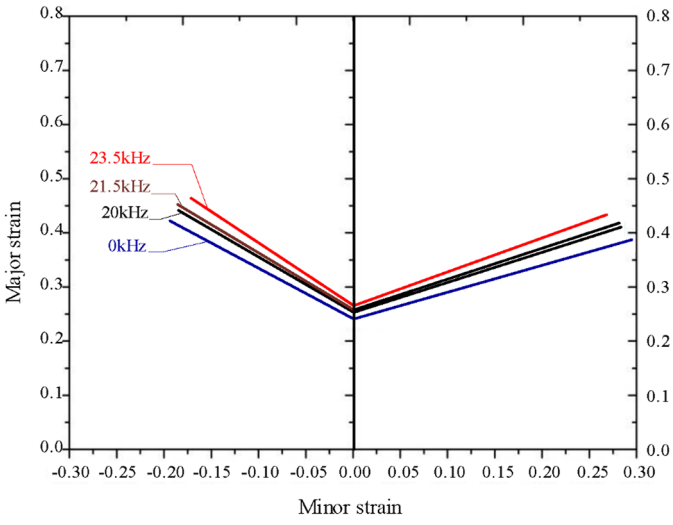

Fig. 12. Experimental FLDs based on ultrasonic vibration.

Figure 12 shows that ultrasonic vibration affected both sides of FLDs to different degrees. At the same frequency of ultrasonic vibration, the FLDs on the left side were slightly larger than those on the right side due to the difference in experimental methods. The left side of FLDs was acquired from uniaxial tensile limit forming experiments. Compared with rigid hemispherical punch experiments, the ultrasonic vibration on the left side of FLDs could cause a more significant volume effect [15]. In addition, the FLDs increased with the increase of ultrasonic vibration frequency, but the shapes were basically unchanged.

6 Conclusions

The uniaxial tensile and bulging forming limit experimental system were modified. The effects of ultrasonic vibration on metal sheet forming limit were explored under different specimen sizes and ultrasonic vibration parameters. Then correlations between ultrasonic vibration and metal sheet FLDs were explored, and FLDs under ultrasonic vibration were plotted.

- In uniaxial tensile and bulging experiments, as the vibration frequency rises from 20 to 23.5 kHz, the major limit strain increment increases, and the range of increment is 2–9.3% and 1.9–8.7%, respectively.
- Ultrasonic vibration has different effects on the left and right sides of the FLD. Under the same ultrasonic vibration frequency, the increment of major limit strain at the left side surpasses that at the right side. Therefore, the volume effect occurring in ultrasonic vibration-assisted metal sheet forming is dominant.
- Comparative analysis shows that the FLDs under ultrasonic vibration increase with the increase of vibration frequency, but the shapes are basically unchanged.

Declaration of conflicting interests

The author(s) declared no potential conflicts of interest with respect to the research, authorship, and/or publication of this article.

Acknowledgments. This study is supported by the Natural Science Foundation of Educational Commission of Anhui Province of China (Grant Number. KJ2019A0576).

References

[1] J.C. Hung, C.C. Lin, Investigations on the material property changes of ultrasonic-vibration assisted aluminum alloy upsetting, Mater. Design. **45**, 412–420 (2013)
[2] T. Ma, Y. Segawa, Y. Miyazaki et al., Effects of periodic waveform wrinkles on ultrasonic reflection characteristics in press forming, Proc. Manuf. **15**, 969–975 (2018)
[3] S. Liu, X. Shan, K. Guo et al., Experimental study on titanium wire drawing with ultrasonic vibration, Ultrasonics. **83**, 60–67 (2018)
[4] M. Zarei, M. Farzin, M. Mashayekhi, Investigating the ultrasonic assistance in the tube hydroforming process, J. Appl. Comput. Mech. **3**, 178–184 (2017)
[5] L. Xu, Y. Lei, H. Zhang, et al., Research on the micro-extrusion process of copper T2 with different ultrasonic vibration modes, Metals **9**, 1209 (2019)
[6] D. Banabic, I.R. DöRr, Prediction of the forming limit diagrams in pulsatory straining, J. Mater. Process. Technol. **45**, 551–556 (1994)
[7] D. Banabic, S. Valasutean, The effect of vibratory straining upon forming limit diagrams, J. Mater. Process. Technol. **34**, 431–437 (1992)
[8] N. Najafizadeh, M. Rajabi, R. Hashemi et al., Improved microstructure and mechanical properties of sheet metals in ultrasonic vibration enhanced biaxial stretch forming, J. Theor. Appl. Vib. Acoust. **5**, 1–10 (2019)
[9] M. Gorji, B. Berisha, P. Hora, et al., Modeling of localization and fracture phenomena in strain and stress space for sheet metal forming, Int. J. Mater. Form. **9**, 573–584 (2016)

[10] S.K. Paul, S. Roy, S. Sivaprasad et al., Forming limit diagram generation from in-plane uniaxial and notch tensile test with local strain measurement through digital image correlation, Phys. Mesomech. **22**, 340–344 (2019)
[11] A.S. Taylor, M. Weiss, T. Hilditch et al., Formability of cryo-rolled aluminium in uniaxial and biaxial tension, Mater. Sci. Eng. **555**, 148–153 (2012)
[12] Z. Marciniak, K. Kuczynski, Limit strains in the processes of stretch-forming sheet metal, Int. J. Mech. Sci. **9**, 609–620 (1967)
[13] Q.T. Pham, B.H. Lee, K.C. Park et al., Influence of the post-necking prediction of hardening law on the theoretical forming limit curve of aluminium sheets, Int. J. Mech. Sci. **140**, 521–536 (2018)
[14] S. Holmberg, B. Enquist, P. Thilderkvist, Evaluation of sheet metal formability by tensile tests, J. Mater. Process. Technol. **145**, 72–83 (2004)
[15] C.L. Zha, W. Chen, Theories and experiments on effects of acoustic energy field in micro-square cup drawing, Int. J. Adv. Manuf. Technol. **104**, 4791–4802 (2019)

Cite this article as: C. Zha, S. Zha, Experimental study on influence of ultrasonic vibration on forming limit, Mechanics & Industry **23**, 14 (2022)